Rev. Fac. Ing. Univ. Antioquia N. º74 pp. 117-131, March, 2015

Design, modeling and dynamic simulation of three double stage gearboxes with different module, mesh stiffness fluctuation and different level tooth breakage

Diseño, modelado y simulación dinámica de tres cajas de engranajes de doble etapa con modulo diferentes, fluctuación de la rigidez de engrane y diferentes niveles de ruptura del diente

Jairo Alberto Ruiz-Botero, Juan Fernando López-López, Héctor Fabio Quintero-Riaza[*]

Facultad de Ingeniería Mecánica, Universidad Tecnológica de Pereira. Vereda la Julita. C.P. 660003. Pereira, Colombia.

(Received April 09, 2014; accepted August 26, 2014)

Abstract

This paper presents the detection of failure in gears using, as a statistical indicator, the Root Mean Square value from the vibration residual signal. Models for three double stage gearboxes are considered on the analysis. The gear models are designed with different modules in order to preserve geometrical resemblance. This research shows the variation on gear mesh stiffness for different amounts of damage. This paper also describes the development of a model to simulate the vibration response from the double stage gearbox for conditions with and without failure. The variation on time of the gear mesh stiffness is taken into account on the dynamic simulation, and damping coefficient is considered proportional to gear mesh stiffness. Results obtained from dynamic simulation for both good state and with failure teeth are in accordance with the results reported on literature.

----------*Keywords:* Gear mesh stiffness, residual signal, breakage of tooth, dynamic response

Resumen

Este artículo utiliza el valor RMS de la señal residual de vibración como indicador estadístico que permita detectar la falla en ruedas dentadas. En el análisis se consideran tres modelos de caja de engranajes de doble

[*] Corresponding author: Héctor Fabio Quintero Riaza, e-mail: hquinte@utp.edu.co

etapa diseñados con diferentes módulos buscando conservar semejanzas geométricas. En este trabajo se muestra la variación de la rigidez de engrane para diferentes tamaños de daño. Se desarrolla un modelo para simular la respuesta de vibración de la caja de engranajes de dos etapas para condiciones de buen estado y con falla. En la simulación dinámica se considera la rigidez de engrane variante en el tiempo y el coeficiente de amortiguamiento se considera proporcional a la rigidez de engrane. Los resultados obtenidos de la simulación dinámica para los dientes en buen estado y con falla son acordes con los reportados en la literatura.

----------*Palabras clave:* Rigidez de engrane, señal residual, ruptura del diente, respuesta dinámica

Introduction

Whether it is in the industrial machinery, automotive applications, or in our daily lives, gearboxes are the most important mechanisms for mechanical power transmission. They provide rotational speed changes and/or change the direction of motion [1], even in an unfavorable working condition, such as lubrication or an assembly problem. This tends to produce fatigue and over-stress, leading to deformation or material loss on teeth, which is reflected in lack of tooth's stiffness -that is proportional to its damage-, affecting the system dynamical response, and showing changes on system's vibration and louder acoustic emissions by internal excitations from cyclic time-varying mesh stiffness. Gear transmission modeling with failure can help in the analysis of this dynamical change in order to obtain adequate results allowing the maintenance personnel to monitor gearbox health, and to detect early faults [2]. In the literature there are many papers related to gearbox modeling in order to obtain a dynamical response.

The mathematical model is used in gear dynamics up to 1986 [3]. A widely used model expresses all the basic factors: design, production technology, operation and change of gear system condition [4]. This model has a bearing to reduce the vibration generated by the gearset, and can be researched using computational simulation inferring diagnostic information of the gearing system. In [5] a model is presented to study the effects of dynamic response for one-stage gear with different teeth. Statistical indicators have been assessed to detect cracks growth [1, 6], with satisfactory results.

The purpose of this paper is the development of a model for a double stage gearbox with involute teeth. Its input torque is constant and its output torque is proportional to the square of the speed, considering mesh stiffness fluctuation and damping coefficient proportional to teeth pairs meshing stiffness. This research pretends to assess the efficiency of RMS value from a residual signal as a statistical indicator for a double stage gearbox system designed with a different module gear mesh. Three double stage gearboxes with geometrical resemblance were designed in order to assess the statistical indicator.

Involute tooth profile is generated by the equations developed in [7]. This profile will be used to posterior calculations of gear meshing. The stiffness of one tooth is calculated from the deflection due to bending, contact and fillet-foundation deflections. Deflection due to bending is based on an analytical equation system shown in [8]. Fillet-foundation deflection considers the model developed in [9]. Afterwards, gear stiffness time variation is calculated analytically for gear with and without damage based on [1, 5, 6, 10].

Finally, model-construction equations are showed for the system based on standard Lagrangian equation, and the dynamical response is calculated. From this the analytical model

frequency domain is obtained, which is compared to results presented by other authors, which verifies the model capacity to reflect the effects of a breakage tooth in dynamical response.

Design of the double stage gearboxes

Three gearboxes were designed with different modules under AGMA standard [11]. The design of the three gearboxes aims to preserve the geometrical resemblance of reducers. The design has the following constraints:

- Stress resilience S_{fb}' and bending safety factor N_b is the same for the first and second stage gears.
- Gears from the reducers have the same number of teeth, which guarantees the gear ratio.
- Wheel width from first stage is given by W_1=8 m_1, where m_1 is the module for the first step.
- Wheel width for the second stage is given by W_2=19 m_2, where m_2 is the module for the second step.
- For a k-gear between different reducers, relationship between dedendum circle radio $r_{f,k}$ and its shaft radio $h=r_{f,k}/r_a$, is constant.

Double stage gears parameters for the three reducers designed that fulfill the previous constraints are given on table 1.

Table 1 Parameters of the double stage gears, for the three reducers

Similar parameters of the three reducers				
	Pinion 1	Gear 1	Pinion 2	Gear 2
Teeth numbers	18	26	20	35
Pressure angle α	20	20	20	20
Coef. Dedendum ϕ	1.4	1.4	1.4	1.4
Coef. Adendum	1	1	1	1
Coef. Tips radius γ	0.35	0.35	0.35	0.35
Cutter offset e	0	0	0	0
Contact ratio c	1.5724	1.5724	1.5724	1.5724
Rotation speed (rpm)	1674	1159	1159	662
Modulus of elasticity *E* (kPa)	206	206	206	206
Additional parameters (first reducer). Input Power = 0.4027 hp				
	Pinion 1	Gear 1	Pinion 2	Gear 2
Module	1.25	1.25	1	1
Teeth width *W* (mm)	10	10	19	19
Shaft diameter (mm)	10	10	10	10
Torque (Nm)	1.71	-2.47	-2.47	4.33
Mass (kg)	0.0246	0.0583	0.0345	0.1306
Constant of scale for damping		μ_1=1.2687 exp -6, μ_2=1.4878 exp-6		
Average mesh stiffness (N/m)		$\bar{K}_{12}$=1.9895 exp 8, $\bar{K}_{34}$=3.9312 exp 8		
Bearing stiffness (N/m)		$k_{x1}=k_{y1}=k_{x2}=k_{y2}=k_{x3}=k_{y3}$=3.6862 exp 8		
Torsional stiffness of shaft		k_{s1}=3.8 exp 3		

Additional parameters (second reducer). Input Power = 3.165 hp				
	Pinion 1	Gear 1	Pinion2	Gear2
Module	2.5	2.5	2	2
Teeth width *W* (mm)	20	20	38	38
Shaft diameter (mm)	10	10	10	10
Torque (Nm)	13.46	-19.45	-19.45	34.03
Mass (kg)	0.1966	0.4662	0.276	1.045
Constant of scale for damping		μ_1=2.6122 exp -6, μ_2=2.3335 exp -6		
Average mesh stiffness (N/m)		K_{12}=3.9719 exp 8, K_{34}= 7.8599 exp 8		
Bearing stiffness (N/m)		$k_{x1}=k_{y1}=k_{x2}=k_{y2}=k_{x3}=k_{y3}$= 6.1075 exp 8		
Torsional stiffness of shaft		k_{s1}= 3.7422 exp 4		
Additional parameters (third reducer). Input Power = 10.546 hp				
	Pinion 1	Gear 1	Pinion2	Gear2
Module	3.75	3.75	3	3
Teeth width W (mm)	30	30	57	57
Shaft diameter (mm)	30	30	30	30
Torque (Nm)	44.86	-64.8	-64.8	113.4
Mass (kg)	0.6635	1.5733	0.9316	3.527
Constant of scale for damping		μ_1= 3.9136 exp -6, μ_2= 3.4997 exp -6		
Average mesh stiffness (N/m)		K_{12}= 5.9719 exp 8, K_{34}= 1.1794 exp 9		
Bearing stiffness (N/m)		$k_{x1}= k_{y1}= k_{x2}= k_{y2}= k_{x3}= k_{y3}$= 8.59 exp 8		
Torsional stiffness of shaft		k_{s1}=1.3281		

Designing under AGMA standard demands that gear teeth could resist fracture by both bending and tooth superficial stresses [12]. According to this, speed reducer gear mesh are designed from AISI 4340 steel values, considering a bending breakage safety factor N_b=3 for first and second step gear, respectively; and it was checked that superficial stress safety factor was greater than one N_c>1.

Bending safety factor for each gear mesh composing the reducer is given by Eq. (1):

$$N_b = \frac{S_{fb}}{\sigma_b} \tag{1}$$

where S_{fb} is the corrected strength, and σ_b is the bending stress.

The corrected strength S_{fb} is given by Eq. (2):

$$S_{fb} = \frac{K_L}{K_T K_R} S_{fb'} \tag{2}$$

The bending-fatigue strength, S_{fb}', of AISI 4340 is 250 MPa. The values of the factors K_L, K_T and K_R are given in table 2.

Table 2 Factors for the calculations of Eq. (1), Eq. (2), Eq. (8) and Eq. (9) [12]

Factor	
Life factor-bending fatigue	K_L=1
Temperature Factor	K_T= C_T= 1
Reliability factor	K_R= C_R= 1.25
Application factor	K_a= C_a= 1
Load distribution factor	K_m= C_m= 1.6
Size Factor	K_S= C_S= 1
Rim thickness factor	K_B= 1
Idler factor	K_I= 1
Geometry factor [13]	J_{G1} = 0.307, J_{G1} = 0.343, J_{G3} = 0.326, J_{G1} = 0.375
Surface-life factor	C_L= 1
Hardness ratio factor	C_H= 1
Elastic coefficient $MPa^{-0.5}$	C_p= 191
Surface finish factor	C_F= 1

The bending stress σ_b is given by Eq. (3):

$$\sigma_b = \frac{F_t}{WmJ_G}\frac{K_a K_m}{K_v} K_s K_B K_I \quad (3)$$

where F_t is tangential load, W is tooth width, m is the module, K_v is the Dynamic factor. Factors K_a, K_m, K_s, K_B and K_I are given in table 2. The dynamic factor K_v is calculated using Eq. (4).

$$K_v = \left(\frac{A}{A + \sqrt{200\,V_t}}\right)^B \quad (4)$$

where V_t is the speed on pass line in m/s. Factors A y B are calculated by Eq. (5) and Eq. (6), respectively:

$$A = 50 + 56\,(1\text{-}B) \quad (5)$$

$$B = \frac{(12 - Q_v)^{2/3}}{4} \text{ for } 6 \le Q_v \le 11 \quad (6)$$

where Q_v is gear-quality factor, which value was taken as 11 .

The surface fatigue safety factor can be calculated as the quotient of the square of corrected surface strength divided by the square of surface stress for each gear in the mesh [12], and it is given by Eq. (7):

$$N_c = \left(\frac{S_{fc}}{\sigma_c}\right)^2 \quad (7)$$

where S_{fc} is the corrected surface-fatigue strength for gear and σ_c is the pitting resistance. S_{fc}, it is calculated using Eq. (8):

$$S_{fc} = \frac{C_L C_H}{C_T C_R} S_{fc'} \quad (8)$$

where $S_{fc'}$ is surface-fatigue strength published by AGMA, which is 1050 MPa for AISI 4340. C_L, C_H, C_T, and C_R factors are given in table 2. σ_c is the pitting resistence, defined by AGMA by Eq. (9):

$$\sigma_c = C_P\sqrt{\frac{F_t}{WId}\frac{C_a C_m}{C_v} C_s C_f} \quad (9)$$

where, C_a, C_m, C_v, C_s, C_p and C_f factors are given in table 2. d is the pitch diameter for the smallest gear in the mesh. I is the surface geometry factor. AGMA defines an equation for I, Eq. (10):

$$I = \frac{\cos\phi}{\left(\frac{1}{\rho_P} + \frac{1}{\rho_g}\right) d_p} \quad (10)$$

where ρ_p and ρ_g are the radii of curvature for pinion and gear teeth, respectively, φ is the pressure angle, and d_p is the pitch diameter of pinion. The curvature radii for teeth are calculated from mesh geometry using Eq. (11) and Eq. (12):

$$\rho_P = \sqrt{\left(r_p + \frac{1 + x_p}{P_d}\right)^2 - (r_p \cos\phi)^2} - \frac{\pi}{P_d}\cos\phi \quad (11)$$

$$\rho_g = C \sin\phi - \rho_P \quad (12)$$

where p_d is the diametral pitch, r_p is the picth radius of pinion, C is the center distance between gear and pinion, and x_p is the pinion addendum coefficient, which is equal to decimal percentage of addendum elongation for unequal addendum teeth.

Time variation of gearmesh stiffness

Gearmesh stiffness was calculated for involute teeth. Since this tooth profile is the most used in the industry because of its advantages in comparison to other tooth profile [14]. Tooth profile for each gear of the three gearboxes with characteristics given on table 1, was obtained using the equations developed in [7], which in turn are a combination of parametric equations to generate tooth filet (BC curve) and involving profile (AB curve), as it can be seen in the figure 1.

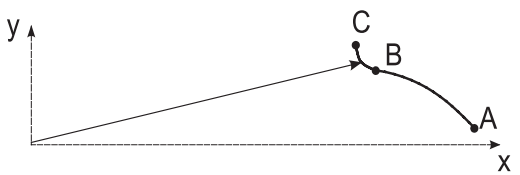

Figure 1 Involute y fillet tooth profiles

The stiffness of one tooth is function of the tooth geometry, the position of the contact point (the bending deflection and fillet-foundation deflection depends of the contact point), gear tooth deflections, gear tooth profile errors, gear hub torsional deformation and finally the local faults on the tooth. On this paper it is calculated from the deflection due to bending, contact and fillet-foundation deflections [10]. This work does not include the analysis of torsional mesh stiffness.

The deflections of a spur tooth gear can be determined by considering it as a non-uniform cantilever beam as shown in the figure 2.

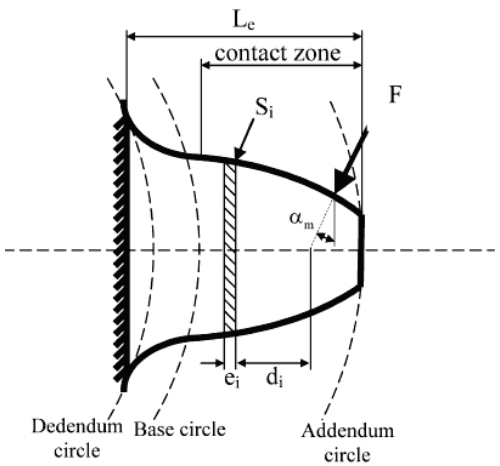

Figure 2 Model of the spur gear tooth as a non-uniform cantilever for bending deflection computation [8]

The bending deflection, δ_b, of a tooth is computed using the model shown in [8], is giving by Eq. (13).

$$\delta_b = F\cos^2\alpha_m \sum_{i=1}^{n} e_i \left\{ \frac{\left(d_i - e_i d_i + \frac{1}{3}e_i^2\right)}{E'\bar{I}_i} + \frac{1}{s_h G \bar{A}_i} + \frac{\tan^2\alpha_m}{\bar{A}_i E'} \right\} \quad (13)$$

where F is the applied force, α_m is the operating pressure angle, s_h is a shear factor, G is the shear modulus, d_i and e_i are given in the figure 2. E', $\bar{I}_i$ and $\bar{A}_i$ are expressed by Eq. (14), Eq. (15) and Eq. (16), respectively:

$$E' = \frac{E(1-\mu)}{(1+\mu)(1-2\mu)} \quad (14)$$

$$\frac{1}{\bar{I}_i} = \frac{\frac{1}{I_i} + \frac{1}{I_{i+1}}}{2} \quad (15)$$

$$\frac{1}{\bar{A}_i} = \frac{\frac{1}{A_i} + \frac{1}{A_{i+1}}}{2} \quad (16)$$

where I_i is the area moment of inertia and A_i is the area of the tooth cross section. E is the Young modulus, and μ is the Poisson's ratio.

The bending stiffness of the tooth on load application point can be obtained using Eq. (17):

$$k_b = \frac{F}{\delta_b} \quad (17)$$

From the results derived in [15], the stiffness of Hertzian contact of two meshing teeth is practically constant along the entire line of action independent from the position of contact and the depth of interpenetration. The stiffness of contact k_h is given by Eq. (18)

$$k_h = \frac{\pi E W}{4(1-\mu^2)} \quad (18)$$

where W is the tooth width.

Besides the tooth deformation, the fillet-foundation deflection also influences the stiffness of gear tooth. In [9] is derived the fillet-foundation deflection of the gear based on the theory shown in [16] applied to circular elastic rings, which assumes linear and constant stress variations at the root circle. It can be calculated using Eq. (19):

$$\delta_f = \frac{F\cos^2\alpha_m}{WE} \left\{ \begin{matrix} \dot{L}\left(\frac{u_f}{S_f}\right)^2 + \dot{M}\left(\frac{u_f}{S_f}\right) \\ +\dot{P}(1+\dot{Q}\tan^2\alpha_m) \end{matrix} \right\} \quad (19)$$

Where u_f and S_f are given in figure 3.

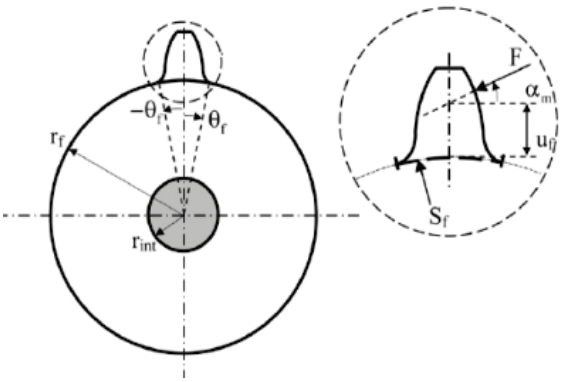

Figure 3 Geometrical parameters for the fillet-foundation deflection [9]

The coefficients L^*, M^*, P^* y Q^* can be approached by polynomial functions [9], using Eq. (20):

$$\dot{X}_i(h_{fi},\theta_f) = \frac{A_{Gi}}{\theta_f^2} + B_i h_{fi}^2 + \frac{C_i h_{fi}}{\theta_f} + \frac{D_i}{\theta_f} + E_i h_{fi} + F_i \quad (20)$$

$h_{fi} = r_f / r_{int}$, r_f, r_{int} and θ_f are defined in figure 3, the values of A_{Gi}, B_i, C_i, D_i, E_i and F_i are given in table 3.

Table 3 Coefficient values for Eq. (20) [9]

	A_{Gi}	B_i	C_i	D_i	E_i	F_i
$\dot{L}(h_{fi}, \theta_f)$	-5.5574 x 10^{-5}	-1.9986 x 10^{-3}	-2.3015 x 10^{-4}	4.77021 x 10^{-3}	0.0271	6.8045
$\dot{M}(h_{fi}, \theta_f)$	60.111 x 10^{-5}	28.100 x10^{-3}	-83.431 x 10^{-4}	-9.9256 x 10^{-3}	0.1624	0.9086
$\dot{P}(h_{fi}, \theta_f)$	-50.952 x 10^{-5}	185.50 x 10^{-3}	0.0538 x 10^{-4}	53.300 x 10^{-3}	0.2895	0.9236
$\dot{Q}(h_{fi}, \theta_f)$	-6.2042 x 10^{-5}	9.0889 x 10^{-3}	-4.0964 x 10^{-4}	7.8297 x 10^{-3}	-0.1472	0.6904

The stiffness with consideration of gear fillet-foundation deflection can be obtained by Eq. (21)

$$k_f = \frac{F}{\delta_f} \quad (21)$$

Gearmesh stiffness, K_e, for a one pair of teeth at a desired contact position is obtained using a serial combination of stiffness: the obtained bending stiffness of the tooth k_b, fillet-foundation stiffness of the tooth k_f, and the stiffness of Hertzian contact of two meshing teeth k_h. It can be written using Eq. (22):

$$K_e = 1/\left(\frac{1}{k_{b1}} + \frac{1}{k_{f1}} + \frac{1}{k_{b2}} + \frac{1}{k_{f2}} + \frac{1}{k_h}\right) \quad (22)$$

Subscripts 1 and 2 denote respectively the pinion and the gear.

Figure 4a shows the typical gearmesh stiffness variation during teeth engagement [15]. Figure 4b is the time varying gearmesh stiffness $Ke(t)$, computed by means of the sum gearmesh stiffness of each pair of teeth in contact. The maximum values of stiffness corresponding to two pairs of teeth in contact are obtained from (nTe) to (c − 1) (nTe), and the minimum values corresponding to one pair in contact are obtained from (c − 1)(nTe)to ((n + 1)Te) with n integer [17], since c is the contact ratio and Te is the gearmesh period (in seconds).

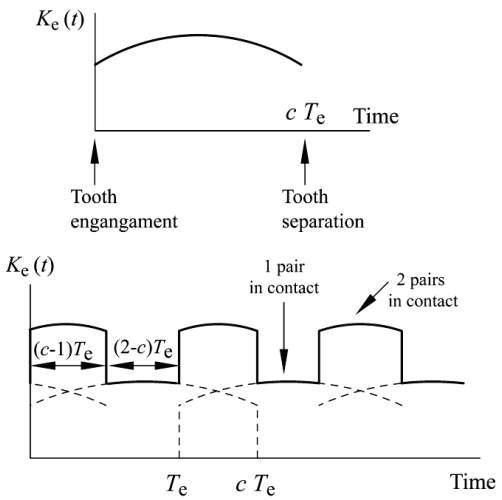

Figure 4 a) Typical variation of the gearmesh stiffness from tooth engagement to separation; b) Time varying gearmesh stiffness computation

Considering a rotational speed ω_1 of the pinion with Z_1 teeth, T_e is defined by Eq. (23):

$$T_e = 60/\omega_1 Z_1 \quad (23)$$

Fault description

In this paper, breakage is the fault modelled. Breakage is the fracture of a whole tooth or substantial part of a tooth. Common causes include overload and cyclic stressing of the gear tooth material beyond its endurance limit. Random fracture can occur in areas such as the top or the end of a tooth, rather than the usual root fillet section [5]. The breakage model studied in this paper, shown in figure 5, causes loss of contact between teeth.

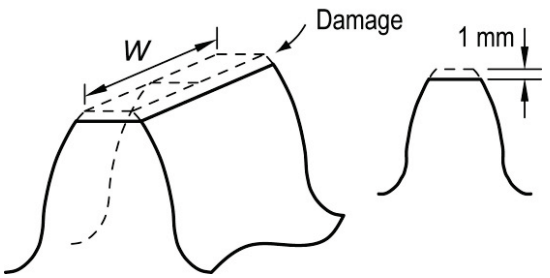

Figure 5 Schematic graph of breakage

Due to this loss of contact, gearmesh stiffness is considered zero during this condition, figure 6a. Figure 6b shows the same effect of this contact loss in the whole gearbox.

If in a pair of teeth occur contact loss for a particular time t_f, shorter than T_e (gearmesh period), the gearmesh stiffness function is zero from t_f to T_e. The two pair of teeth gearmesh stiffness function is reduced, and impact load affects the second pair of teeth. Figure 7 represents the Time-varying mesh stiffness evolution with different breakage height, for three gearboxes. Stiffness calculations for a pair of involute spur teeth, whose main parameters were given in table 1, considering 0%, 2%, 5%, 10%, 15%, 20%, 30%, 40%, 50%, 60% and 70% addendum tooth breakage, were done. According with results, Time-varying mesh stiffness has the typical shape gearmesh which maximum stiffness values corresponding to two pairs in contact, and the minimum values corresponding to one pair in contact [17].

This variation is considered as the gearbox main source of excitation and yields vibration and acoustic emissions [18]. A stiffness reduction is observed for the breakage cases. Since teeth lose contact due to breakage tooth, a stiffness decrease took place. Therefore, mesh stiffness Time-varying calculations are made in advance from two pairs in contact to one pair in contact on breakage zone.

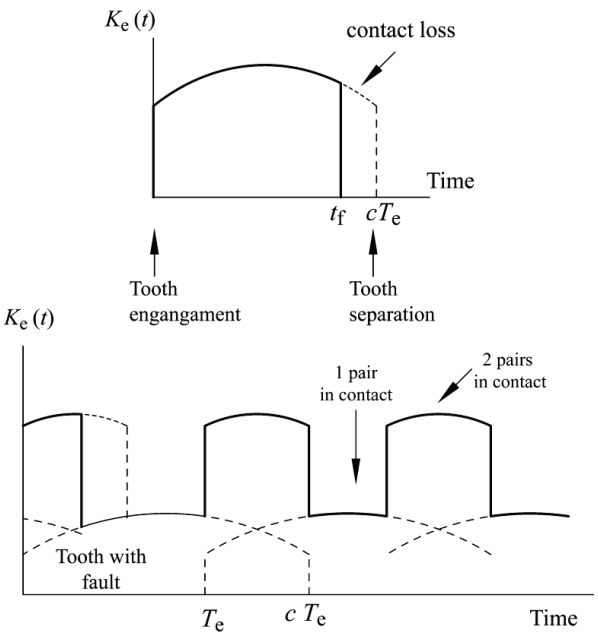

Figure 6 a) Gearmesh stiffness with fault b) Time gearmesh stiffness in breakage case

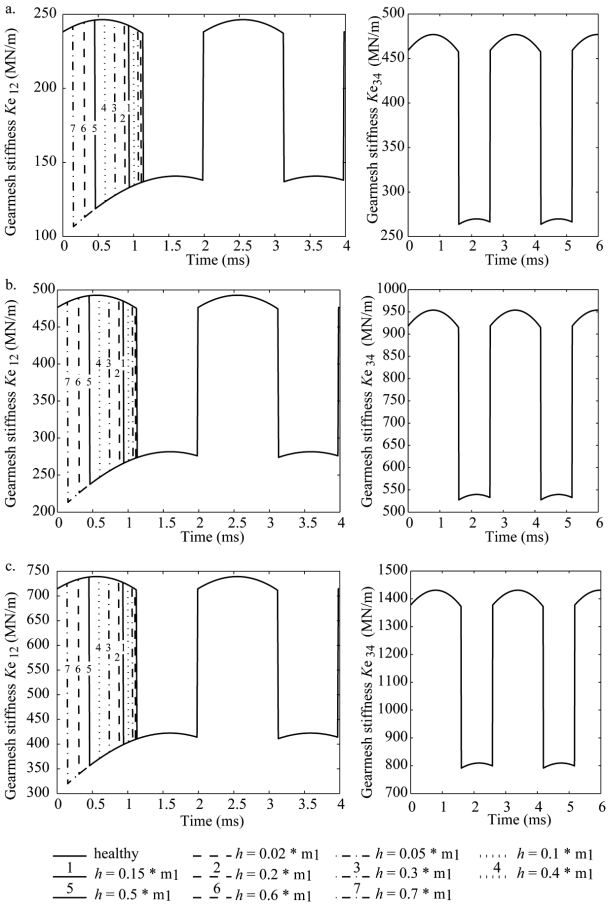

Figure 7 Time-varying mesh stiffness evolution with different breakage height. (a) first gearbox, (b) second gearbox and (c) third gearbox

Modeling of double stage gear trains

The model developed here is based on double stage gear trains (figure 8). The Input torque is constant, T_{in}=cte, and output torque is proportional to the square of the speed, $T_{out} = c\dot{\theta}_3^2$. Gears are modeled as rigid disk with radius equal to the base circle.

The input and output shafts are assumed rigid, while allowed intermediate shaft torsion is represented by the equivalent torsion spring constant. Each shaft is supported by bearings modeled by two linear springs. This implies the simplifying assumption that the gear may move laterally but do not tilt. Gear teeth are flexible, then gearmesh stiffness k_{12} (t) and k_{34} (t) from first and second step, respectively, are modelled by linear spring, acting on the line of action of the meshing teeth, and damping. Gear teeth are assumed to be perfectly involute and manufacturing and assembly errors are ignored. The casing is assumed to be rigid. Tooth separation is not considered. In this study, we assume that the system has a constant damping ratio ς=0.07 [19]. The damping coefficient, c_t, is assumed to be proportional to the meshing stiffness of the tooth pairs. The damping can be considered an improvement of the constant damping factor acting on the velocity and can be considered quite realistic [20] and are given by Eq. (24) and Eq. (25)

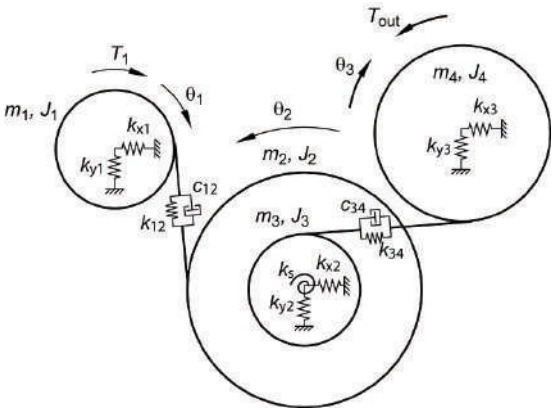

Figure 8 Model of double stage gear system with ten degrees of freedom

$$c_{t1} = \mu_1 k_{12}(t) \quad (24)$$

$$c_{t2} = \mu_2 k_{34}(t) \quad (25)$$

where μ_1 and μ_2 are the constant scale measured in seconds from first and second step, respectively [21]. These parameters of the gearbox system are listed in table 1.

The expression of the displacement on the line of action, giving in [22], is expressed by Eq. (26):

$$\delta(t) = R_p\theta_p - R_r\theta_r - (y_p - y_r)\cos\alpha + (x_p - x_r)\sin\alpha \quad (26)$$

The equations of motion for the model were obtained using the standard Lagrangian equation [23], it is given by Eq. (27):

$$\frac{d}{dt}\left(\frac{\partial T}{\partial \dot{\boldsymbol{q}}_{\boldsymbol{i}}}\right)-\frac{\partial T}{\partial \boldsymbol{q}_{\boldsymbol{i}}}+\frac{\partial V}{\partial \boldsymbol{q}_{\boldsymbol{i}}}+\frac{\partial D}{\partial \dot{\boldsymbol{q}}_{\boldsymbol{i}}}=\boldsymbol{Q}_{\boldsymbol{i}} \quad (27)$$

where $\boldsymbol{q}$ is the vector of degrees of freedom, it is given by Eq. (28):

$$q=\{x_1, y_1, \theta_1, x_2, y_2, \theta_2, \theta_3, x_3, y_3, \theta_4\}^T \quad (28)$$

T is the kinetic energy of the system, given by Eq. (29) and Eq. (30):

$$T_1=\frac{1}{2}(J_1\dot{\theta}_1^2+m_1\dot{x}_1^2+m_1\dot{y}_1^2+J_2\dot{\theta}_2^2+m_2\dot{x}_2^2+m_2\dot{y}_2^2) \quad (29)$$

$$T_2=\frac{1}{2}(J_3\dot{\theta}_2^2+m_3\dot{x}_2^2+m_3\dot{y}_2^2+J_4\dot{\theta}_3^2+m_4\dot{x}_3^2+m_4\dot{y}_3^2) \quad (30)$$

V is the change in potential energy, which is given by:

Variation of the gearmeshes, Eq. (31) and Eq. (32):

$$V_{m1}=\frac{1}{2}K_{12}(t)\langle R_1\theta_1-R_2\theta_2-(y_1-y_2)\cos\alpha+(x_1-x_2)\sin\alpha\rangle^2 \quad (31)$$

$$V_{m2}=\frac{1}{2}K_{34}(t)\langle R_3\theta_2-R_4\theta_3-(y_2-y_3)\cos\alpha+(x_2-x_3)\sin\alpha\rangle^2 \quad (32)$$

Twisting of gear shafts, given by Eq. (33):

$$V_s=\frac{1}{2}k_{s1}(\theta_3-\theta_2) \quad (33)$$

where k_{s1}, intermediate shafts torsional stiffnesses, are given on table 1.

Lateral deflection of bearings can be obtained using Eq. (34):

$$V_{sl}=\frac{1}{2}\left(k_{x1}x_1^2+k_{y1}y_1^2+k_{x2}x_2^2+k_{y2}y_2^2+k_{x3}x_3^2+k_{y3}y_3^2\right) \quad (34)$$

where k_{xi}, k_{yi} (i = 1, 2, 3, 4) are the bearings stiffness, which were calculated on [24]. These are shown on table 1.

D is dissipation function, which are given by Eq. (35) and Eq. (36):

$$D_1=\frac{1}{2}\mu_1K_{12}(t)(R_1\dot{\theta}_1-R_2\dot{\theta}_2-(\dot{y}_1-\dot{y}_2)\cos\alpha+(\dot{x}_1-\dot{x}_2)\sin\alpha)^2 \quad (35)$$

$$D_2=\frac{1}{2}\mu_2K_{34}(t)(R_3\dot{\theta}_3-R_4\dot{\theta}_4-(\dot{y}_2-\dot{y}_3)\cos\alpha+(\dot{x}_2-\dot{x}_3)\sin\alpha)^2 \quad (36)$$

$\boldsymbol{Q}_{\boldsymbol{i}}$ is the external applied forces, it is given by Eq. (37):

$$\boldsymbol{Q}_{\boldsymbol{i}}=\{0\ 0\ 0\ T_{in}\ 0\ 0\ 0\ -T_{out}\}^T \quad (37)$$

Where T_{out} is obtained using Eq. (38)

$$T_{out}=c_f\dot{\theta}_3^2 \quad (38)$$

The proportionality constant, c_f, is given by Eq. (39):

$$c_f=\frac{T_{in}Z_2^3Z_4^3}{Z_1^3Z_3^3\dot{\theta}_{in}^2} \quad (39)$$

where $\dot{\theta}_{in}$(rad/s) and T_{in} (Nm) is nominal speed and input torque, respectively.

Once Lagrangian formulation is applied, system movement equation is obtained, given by Eq. (40):

$$M\ddot{q}+C(t)\,\dot{q}+K(t)q=Q_i \quad (40)$$

where $\boldsymbol{M}$ is a diagonal mass matrix; the matrix $\boldsymbol{K}(t)$ includes the bearings stiffness, torsional stiffness of intermediate shafts and the time varying gearmesh stiffness; and the matrix $\boldsymbol{C}(t)$

includes damping constants and is assumed to be proportional to the meshing stiffness of the tooth pairs. Reformulating the second-order system Eq. (40) into the so-called *state-space* formulation, Eq. (41) is obtained:

$$\dot{y} = \begin{bmatrix} 0 & I_{10x10} \\ -M^{-1}K(t) & -M^{-1}C(t) \end{bmatrix} y + \begin{bmatrix} Zeros_{10x1} \\ M^{-1}Q_i \end{bmatrix} \quad (41)$$

Gear system dynamic response

The dynamic response [25] of the three Gearboxes given by the equation of motion (Eq. (41)) were obtained using the ODE15s Matlab function to extract the displacement, velocity and acceleration of the gear system under health and fault states.

Figure 9 shows the spur gear dynamic response in the three stage gear transmission. X direction displacements of faulty pinion are reflected in figures 9b, 9c y 9d.

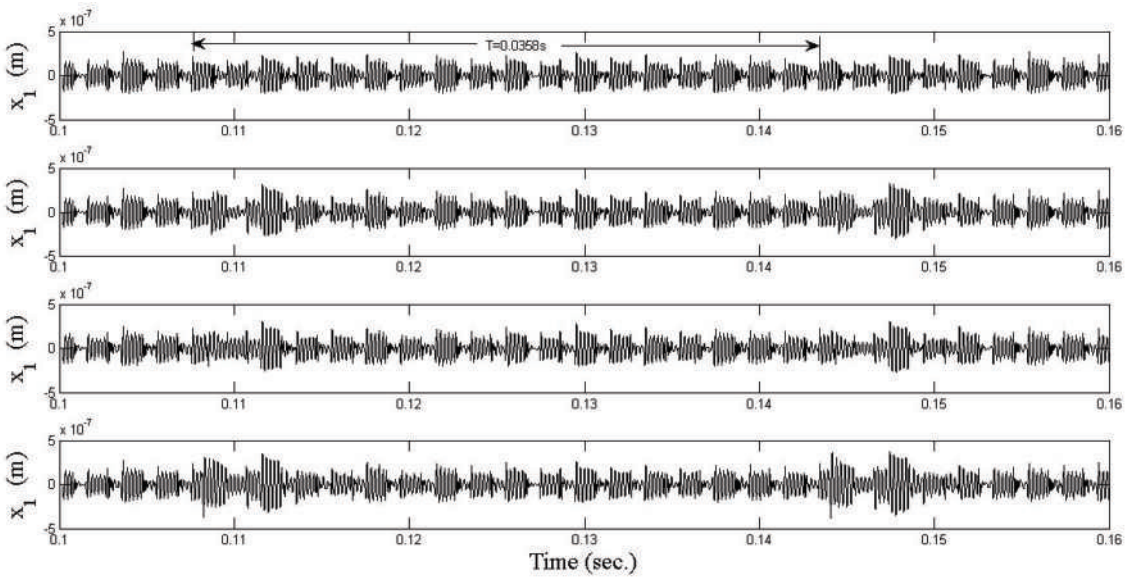

Figure 9 X direction displacement, pinion with fault: (a) 0% breakage, (b) 5% breakage, (c) 20% breakage, (d) 40% breakage

Residual signals

The idea of residual signal was first presented in a local gear fault, such as crack in a tooth [26]. The vibration signal in this fault is modified for a complete revolution by effects of short duration impact impulse. In order to effectively detect the fault features in the vibration signal, the regular components need to be removed; the rest is called the residual signal, which is supposed to be more sensitive to crack growth. Residual signal on this work is determined through the methodology based on idea of removing regular components in signal, which are redundant for the purpose of fault detection, proposes the generation of residual signal, removing the whole original signal of the healthy case from the original signal of the faulty case [1].

Figure 10 shows the dynamic response (in frequency domain) of first stage gear trains (table 1) registered on the input pinion in the direction. Figure 10a is the dynamic response of the healthy case. This figure is characterized for the presence of several dominant peaks which

correspond to the two gearmesh frequencies f_{e1} = 502 Hz, f_{e2} = 386 Hz, and their first harmonics. The figure 10b is the dynamic response (in the frequency domain) of the defected case with 10% of breakage of input pinion. In the defected cases, compared to the healthy case, is observed the appearance of sidebands spaced by the rotational frequency f_1 of the faulty pinion, around gearmesh f_{e1}. These frequencies are analytically given by (n, m integers). Figure 10c is the residual signal obtained using the dynamic response of the healthy case (figure 10a), and the response of the defected case (figure 10b), in figure 10c the sidebands produced by the fault are shown.

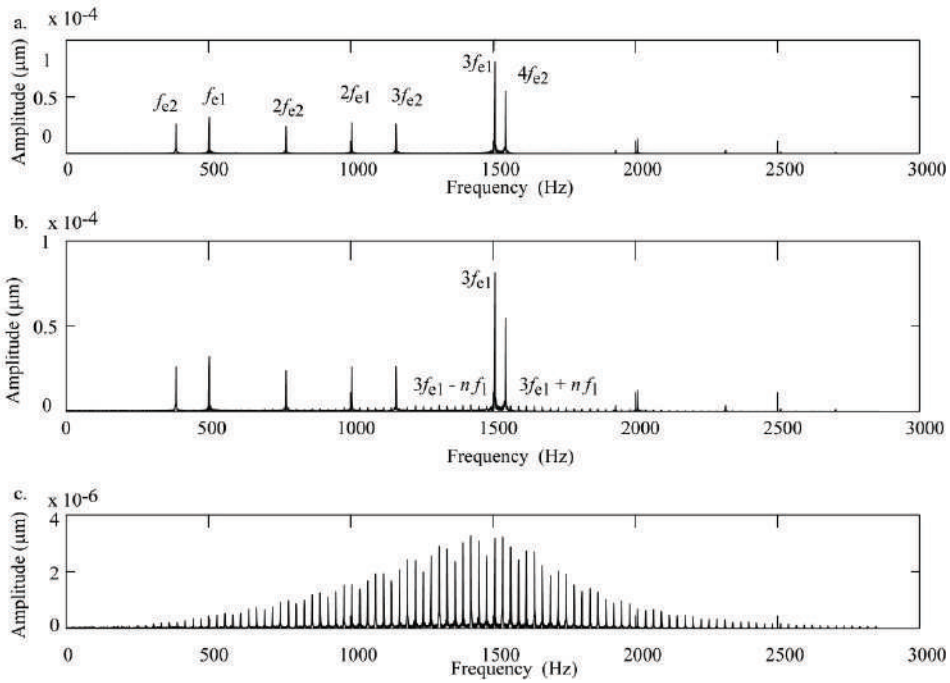

Figure 10 Dynamic response spectrum and residual signal for first stage gear transmission (table 1): (a) vibration displacement response in the direction for 0% breakage, (b) vibration displacement response in the direction for 10% breakage, and (c) residual signal

Statistical fault

Diagnosis indicators

In this work the three gear trains were simulated with different tooth breakage levels and the vibration signals was obtained in each case. In order to obtain an approach to the fault condition, an indicator to extract defect features of the vibration signals is required. Statistical indicators in the Time-domain analysis are the most fundamental. We propose to evaluate the statistical indicator RMS, in [1] concludes that this indicator shows the best performance on the proposed method of generating the residual signal.

In the case where the mean value of the signal is not zero, the RMS indicator can be obtained using equations (42) y (43) [27]:

$$RMS = \sqrt{\frac{1}{N}\sum_{n=1}^{N}(x(n) - \bar{x})^2} \quad (42)$$

$$\bar{x} = \frac{1}{N}\sum_{n=1}^{N} x(n) \quad (43)$$

The residual signal of the acceleration component of the third pair of gears, which parameters are given in table 1, considering the proposed tooth breakage levels in each gear train, was calculated. Figure 11 shows the RMS value for each analyzed signal, the y axis corresponds to the changes of healthy tooth. This figure shows the RMS from residual signal, which allows to detect the appearance of breakage. This can be concluded given the similarity between observed results from the percentage change of RMS for the three pair of gears. On the other side, it was observed that this indicator turns out to be more sensitive to failures up to 15%, because for major failures bigger changes are not observed.

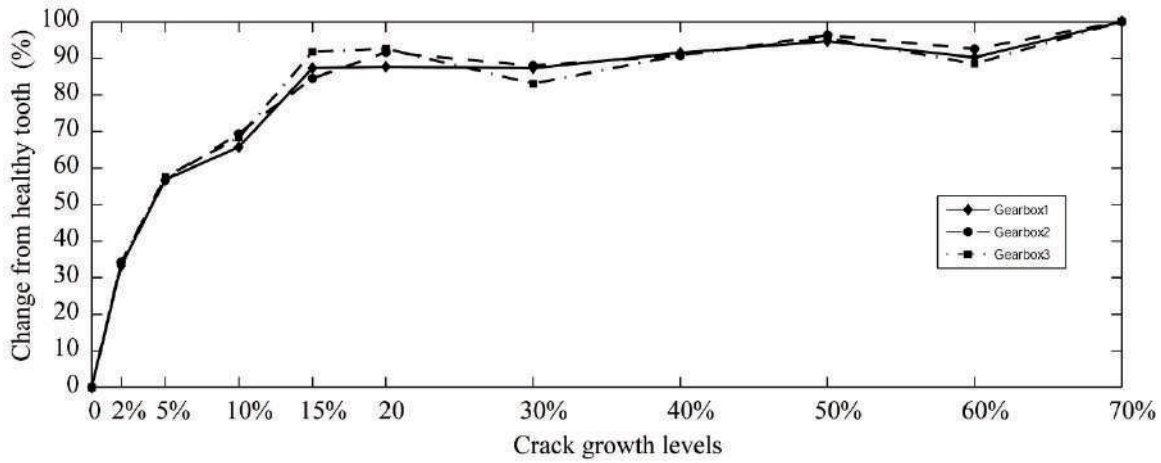

Figure 11 RMS change for three gearbox

The application of this paper is framed within the online identification and monitoring of faults in rotating machinery using the stochastic variability of the vibration signals as the main tool for the characterization of faults.

The creation of a database of vibration signals enables future training algorithms for the subsequent diagnosis of faults in real industrial applications.

Conclusions

In this paper, three double stage gearboxes were designed with different modules. Time-varying mesh stiffness evolution was calculated considering different breakage levels ranging from 0% to 70% of module of tooth. An analytical model was developed for a double stage gearbox with output torque proportional to the square of the speed. Dynamical model simulation was made with stiffness calculated for the gears under different tooth breakage levels on the pinion, and is represented on frequency domain observing the two gearmesh frequencies and as their first harmonics. For gear with failure, lateral band was observed around gear frequency and its harmonics, which are caused for lack of stiffness. These observed lateral bands are in accordance with the results reported on the literature. With the simulated vibration signals, the residual signal is determined. The RMS statistical indicator is evaluated in the three gearboxes to reflect their change on levels of vibration signals obtained of dynamical response with tooth breakage. It has been found that the RMS of the residual signal is an effective indicator of the gears conditions for detects the appearance of teeth breakage in at wo-stage gearbox; it will be used to diagnose presence of failure.

Acknowledgment

The authors acknowledge the support given at this work by Colciencias, by means of contract RC 472-2011, code 111052128503 to the research group in Procesos de Manufactura y Diseño de Máquinas of the Universidad Tecnológica de Pereira, which made possible this work.

References

1. S. Wu, M. Zuo, A. Parey. "Simulation of spur gear dynamics and estimation of fault growth". *Journal of Sound and Vibration*. Vol. 317. 2008. pp. 608-624.

2. P. Chen, F. Feng, T. Toyota. *Dynamic analysis method of fault gear equipment*. Proceedings of the 14th International Congress on Condition Monitoring and Diagnostic Engineering Management (COMADEM). Manchester, UK. 2001. pp. 419-426.

3. H. Özgüven, D. Houser. "Mathematical Models Used in Gear Dynamics - A Review". *Journal of Sound and Vibration*. Vol. 121. 1988. pp. 383-411.

4. W. Bartelmus. "Mathematical modelling and computer simulations as an aid to gearbox diagnostics". *Mechanical Systems and Signal Processing*. Vol. 15. 2001. pp. 855-871.

5. F. Chaari, T. Fakhfakh, M. Haddar. "Effect of spalling or tooth breakage on gearmesh stiffness and dynamic response of a one-stage spur gear transmission". *European Journal of Mechanics A/Solids*. Vol 27. 2008. pp. 691-705.

6. Z. Chen, Y. Shao. "Dynamic simulation of spur gear with tooth root crack propagating along tooth width and crack depth". *Engineering Failure Analysis*. Vol. 18. 2011. pp. 2149-2164.

7. J. Wang. *Numerical and Experimental Analyses of Spur Gears in Mesh.* Ph.D Thesis, Curtin University of Technology. Sidney, Australia. 2003. pp. 49-64.

8. C. Weber. *The deformation of loaded gears and the effect on their load-carrying capacity*. Report N.° 3, Sponsored research (Germany), British Dept. of Sci. and Ind. Res. London, UK. 1949. pp. 22.

9. P. Sainsot, P. Velex, O. Duverger. "Contribution of gear body to tooth deflections – a new bidimensional analytical formula". *ASME J. Mec.Des*. Vol. 126. 2004. pp. 748-752.

10. F. Chaari, T. Fakhfakh, M. Haddar. "Analytical modeling of spur gear tooth crack and influence on gearmesh stiffness". *European Journal of Mechanics A/Solids*. Vol. 28. 2009. pp. 461-468.

11. American Gear Manufacturers Association. *Fundamental Rating Factors and Calculation Methods for Involute Spur and Helical Gear Teeth*. ANSI/ AGMA 2001-B88. Alexandria, USA. 2001. pp. 58

12. R. Norton. *Machine design, an integrated approach*. 4th ed. Ed. Pearson Education, Inc. New Jersey, USA. 2006. pp. 681-746.

13. R. Budynas, J. Nisbett. *Diseño en ingeniería mecánica de Shigley*. 8th ed. Ed. McGraw-Hill/ Interamericana Editores, S. A. de C.V.. Mexico, D. F., Mexico 2008. pp. 713-763.

14. F. Litvin, A. Fuentes. *Gear Geometry and Applied Theory*. 2nd ed. Ed. Cambridge University Press. New York, USA. 2004. pp. 800.

15. D. Yang, Z. Sun. "A rotary model for spur gear dynamics". *ASME J. Mech. Des*. Vol. 107. 1985. pp. 529-535.

16. N. Muskhelishvili. *Some Basic Problems of the Mathematical Theory of Elasticity*. 2nd ed. Ed. Noordhoff International Publishing. Leyden, Netherlands. 1977. pp. 176-196.

17. F. Chaari, T. Fakhfakh, M. Haddar. "Simulation numérique du comportement dynamique d'une transmission par engrenages en présence de défauts de denture". *Mécanique & Industries*. Vol. 6. 2005. pp. 625-633.

18. F. Chaari, T. Fakhfakh, M. Haddar. "Dynamic analysis of a planetary gear failure caused by tooth pitting and cracking". *Journal of Failure Analysis and Prevention*. Vol. 6. 2006. pp. 73-78.

19. S. Harris. "Dynamic Loads on the Teeth of Spur Gears". ARCHIVE: *Proceedings of the Institution of Mechanical Engineers*. Vol. 172. 1958. pp. 87-112.

20. M. Amabili, A. Rivola. "Dynamic analysis of spur gear pairs: steady-state response and stability of the SDOF model with time-varying meshing damping". *Mechanical systems and signal processing*. Vol. 11. 1997. pp. 375-390.

21. X. Tian. *Dynamic Simulation for System Response of Gearbox Including Localized Gear Faults*. M.Sc. Thesis, University of Alberta. Alberta, Canada. 2004. pp. 64-88.

22. F. Chaari, T. Fakhfakh, R. Hbaieb, J. Louati, M. Haddar. "Influence of manufacturing errors on the dynamic behavior of planetary gears". *The International*

Journal of Advanced Manufacturing Technology. Vol. 27. 2006. pp. 738-746.

23. J. Kuria, J. Kihiu. "Modeling parametric vibration of multistage gear systems as a tool for design optimization". *International Journal of Mechanical, Industrial and Aerospace Engineering*. Vol. 2. 2008. pp. 159-166.

24. E. Kramer. *Dynamics of rotors and foundations*. 1st ed. Ed. Springer-Verlag. Berlin, Germany. 1993. pp. 129-141.

25. F. Cellier, E. Kofman. *Continuous system simulation.* 3rd ed. Ed. Springer-Verlag. New York, USA. 2006. pp. 1-478.

26. R. Stewart. *Some Useful Data Analysis Techniques for Gearbox Diagnostics. Applications of Time Series Analysis*. PhD Thesis, University of Southampton. Southampton, UK. 1977. pp. 19-22

27. A. Brandt. *Noise and Vibration Analysis: Signal Analysis and Experimental Procedures*. 1st ed. Ed. *John Wiley & Sons*. New Delhi, India. 2011. pp. 68-69.